

# Gas-phase growth of diameter-controlled carbon nanotubes

Soo H. Kim<sup>1</sup>, Michael R. Zachariah\*

*UMCP/NIST Co-Laboratory for NanoParticle Based Manufacturing and Metrology, University of Maryland, College Park, MD 20742, United States*  
*The National Institute of Standards and Technology, Gaithersburg, MD 20899, United States*

Received 7 June 2006; accepted 8 August 2006

Available online 5 September 2006

## Abstract

We demonstrate gas-phase (aerosol) generation of diameter-controlled carbon nanotubes (CNTs) by employing size-controlled monodisperse nickel nanoparticles produced by the combination of pulsed laser ablation and electrostatic classification. The electrostatic classifier sorted agglomerated mono-area nickel particles, and then a subsequent heating process at  $\sim 1200$  °C created sintered single primary particles with very narrow size distribution. These isolated single primary particles were then sent to an aerosol reactor where free-flight CNTs were grown with acetylene and hydrogen mix at temperature of  $\sim 750$  °C. The resulting CNTs formed in this continuous gas-phase process were found to have a uniform diameter, which is commensurate with the diameter of the size-controlled catalytic nickel particles.

© 2006 Elsevier B.V. All rights reserved.

*Keywords:* Catalysts; Carbon nanotubes; Pulsed laser ablation; Sintering process; Nanoparticles; Electrical mobility classification

## 1. Introduction

Carbon nanotubes (CNTs) have been synthesized using various production methods, where carbon atoms are released from carbon precursor by either arc/laser-assisted high-energy input [1,2] or metal particle-assisted catalytic reaction [3–5] followed by diffusion of the released carbon atoms and subsequent nucleation/growth of nanotubes on a supporting surface. One of the desirable structural parameters for CNTs is the control of nanotube diameter as it is important to optimize the performance of various nanotube-based composite materials [6] and electromechanical devices [7]. In a related work, diameter-controlled CNTs grown on wet chemistry-assisted monodisperse iron particles [8] were successfully synthesized on an oxidized silicon substrate.

With the major advantage of continuous production of high purity CNTs, a number of research groups have conducted gas-phase synthesis of CNTs with the assistance of organometallic precursors and a carbon feedstock [5,9], which is typically

termed as aerosol synthesis or floating catalyst method. Rapid thermal decomposition of organometallic precursors results in the formation of supersaturated metal vapor, in which metal nanoparticles are nucleated and grown by condensation and coagulation processes. Instead of using an organometallic precursor, Vander Wal et al. [10] employed a pulsed laser ablation (PLA) to preform metal catalysts particles so that the formation of metal catalysts can be separated from CNTs' growth. This approach enabled one to explore the effect of hydrocarbon identity and reacting temperature on CNTs' growth. However, in these most previous aerosol CNT production approaches, the size of the metal catalysts formed are ill defined, because the evolution of particles and CNTs occurred simultaneously in a high-temperature reactor, where competition between coagulation and sintering processes of the primary metal particles continuously transform their morphology and size.

In this paper, we demonstrate that gas-phase control of CNTs' diameter can be achieved by controlling the size of metal particles, resulting in a narrow size distribution of the CNT diameter. We have prepared size-selected monodisperse metal particles using a gas-phase electrophoretic device (i.e. electrostatic classifier or differential mobility analyzer) followed by a subsequent sintering process, which is found to be crucial for the

\* Corresponding author.

E-mail address: [mrz@umd.edu](mailto:mrz@umd.edu) (M.R. Zachariah).

<sup>1</sup> Present address: Department of Nanosystem and Process Engineering, Pusan National University, Geumjeong Gu, Pusan, 609-735 Korea.

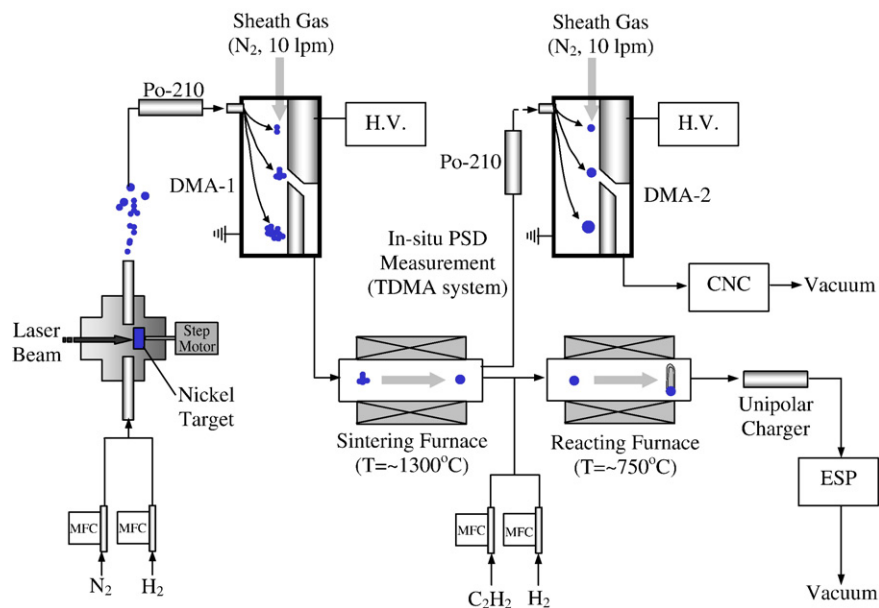


Fig. 1. Schematic of experimental system (DMA: differential mobility analyzer, TDMA: tandem differential mobility analyzer, CNC: condensation nucleus counter, ESP: electrostatic precipitator, MFC: mass flow controller, H.V.: high voltage power supply).

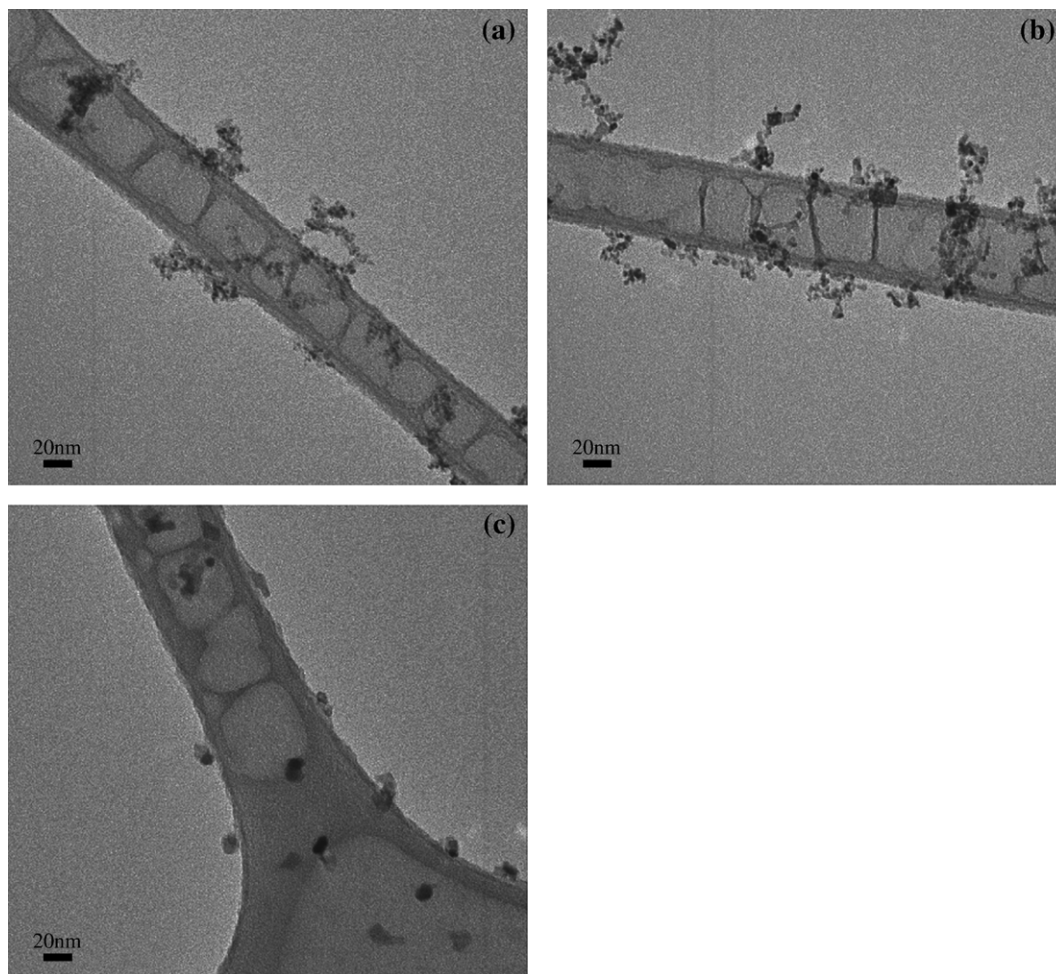


Fig. 2. TEM images of 30 nm mobility size-selected particles followed by sintering at various temperatures of (a) 800 °C, (b) 1000 °C, and (c) 1200 °C.

formation of diameter-controlled CNTs. These size-selected and sintered metal particles catalyze the growth of diameter-controlled CNTs in the gas phase.

## 2. Experimental section

As a catalytic particle source for the growth of CNTs, we chose nickel which was generated by pulsed laser ablation of a solid nickel target, using a 1064 nm Q-switched Nd:YAG laser operating at 10 Hz with a pulse width of 4 ns. The schematic of the pulsed laser ablation method is shown in Fig. 1. The laser beam is focused on the solid nickel target, and it generates a local micro-plasma at the surface of the nickel target, leading to vaporization. A flow of nitrogen was continuously swept past the target surface to carry away the nickel vapor, and cause rapid quenching and nucleation of nickel particles. A small flow of hydrogen gas of  $\sim 50$  sccm was mixed with nitrogen carrier gas to suppress any oxide formation, and was found to make a significant difference in the growth rate and yield of CNTs. The polydisperse metal particles were then rapidly transported into a radioactive ionizing source (Po-210), which produces an equilibrium charge distribution on the metal particles. To classify monodisperse metal particles, a differential mobility analyzer (DMA, Model 3081, TSI, Inc.) was employed as a size selection tool, which is described in detail elsewhere [11,12]. Briefly, when the charged particles are introduced into the DMA, a fraction of particles with same electrical mobility is classified in the balance of electrostatic attraction and drag forces.

For the current study, two DMAs in series were employed: DMA-1 selects out mono-area metal particles, and DMA-2 combined with a condensation nucleus counter (CNC, Model 3025A, TSI, Inc.) connected to the exit of sintering furnace was used to measure the change of size distribution of the DMA-1 classified metal particles following sintering. The CNC counts the particles by growing them via heterogeneous condensation of supersaturated butanol to a size amenable for optical detection. The mono-area metal nanoparticles selected from DMA-1 were sintered at the first tube furnace (hereafter referred to as the sintering furnace) at  $\sim 1300$  °C to form larger unagglomerated primary particles. To grow the CNTs on the sintered metal nanoparticles, acetylene (3–30 sccm) and hydrogen (50–200 sccm) were supplied to the second tube furnace (hereafter as the reacting furnace) at 750 °C. The sintering furnace has 1 in. dia.  $\times$  50 cm heating length and the reacting furnace has 1 in. dia.  $\times$  60 cm heating length so that the residence time was  $\sim 3$  and  $\sim 5$  s at  $\sim 1300$  °C and  $\sim 750$  °C, respectively, for a fixed 1 lpm aerosol flow rate.

The CNTs grown in the gas phase were then passed through a unipolar charger, in which the unipolar ion flow charges the CNTs positively [13]. The positively charged CNTs were then introduced to an electrostatic precipitator (ESP, Model 3089, TSI, Inc.) where a high negative electric field between the charged electrode and grounded chamber forced the positively charged CNTs toward a TEM grid. Following a  $\sim 10$  min deposition time period, the TEM grid was removed for morphological analysis using TEM (Model JEOL 1210, operating at 120 kV).

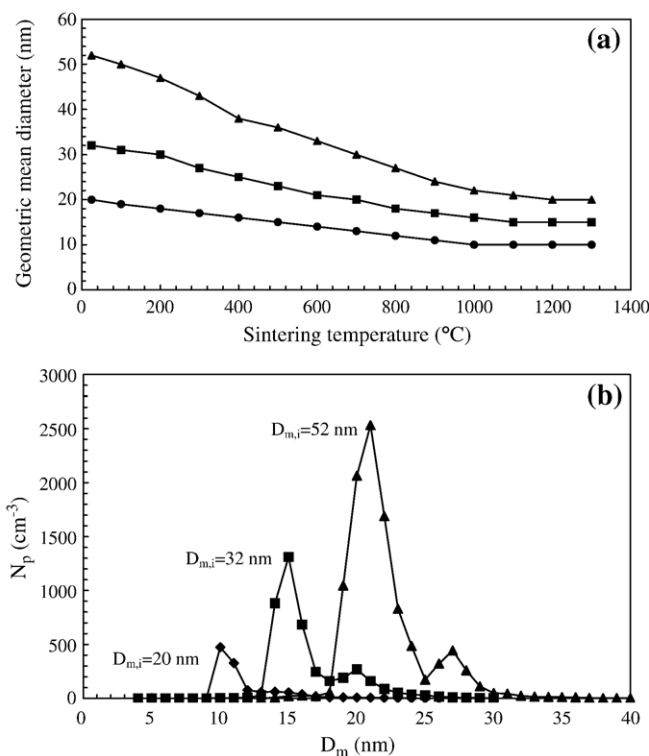


Fig. 3. (a) The evolution of mobility diameter as a function of sintering temperature, (b) size distributions of 1200 °C sintered nickel particles with different initial mobility sizes,  $D_{m,i}$ , selected by an electrostatic classifier (i.e. DMA-1).

### 3. Results and discussion

To control the diameter of primary particles under conditions where they are not agglomerated, we use a size-separation tool and a subsequent high-temperature sintering process for particle size and morphology control, respectively. First, we employ an electrostatic classification with the DMA which (a) creates a continuous stream of narrow mobility diameter particles with equivalent surface area [14], and (b) drops the particle number concentration such that the characteristic coagulation time between particles is lower than the characteristic growth time. The characteristic time for coagulation is calculated as [15],

$$t_{\text{coagulation}} = \frac{2}{KN_0} \quad (1)$$

where  $K$  is the collision kernel (Fuchs form, [16]) under the assumption of monodisperse particles, and  $N_0$  is the number concentration of particles, ( $\sim 10^6 \text{ cm}^{-3}$ ) following electrostatic classification with the DMA. The value obtained is about  $\sim 1000$  s, and is thus much larger than the

experimental residence time of  $\sim 3$  s. This implies that we should grow unagglomerated CNT in free-flight.

Fig. 2 shows TEM images of the 30 nm mobility size-selected nickel particles, which subsequently underwent sintering at various temperatures of 800, 1000, and 1200 °C. As one can see in Fig. 2a, fractal-like agglomerated metal nanoparticles having initial mobility diameter of 30 nm are not fully sintered at  $\sim 800$  °C, even though a simple sintering model calculation would indicate that the particles should be fully sintered [17]. We believe this latter condition is related to the nature of such sintering models, which were not developed for large aggregates containing, as in our case, more than 20 primary particles per aggregate. It is also possible that surface oxide inhibited coalescence, since the growth of CNTs on the mobility-classified nickel particles was found to be promoted by hydrogen addition. The agglomerated primary particles are then partially collapsed to form a larger primary particle when the sintering temperature reaches 1000 °C (see Fig. 2b). A temperature of 1200–1300 °C at our residence times was required to completely sinter so that we can obtain isolated single primary particles having the diameter of  $\sim 15$  nm (Fig. 2c).

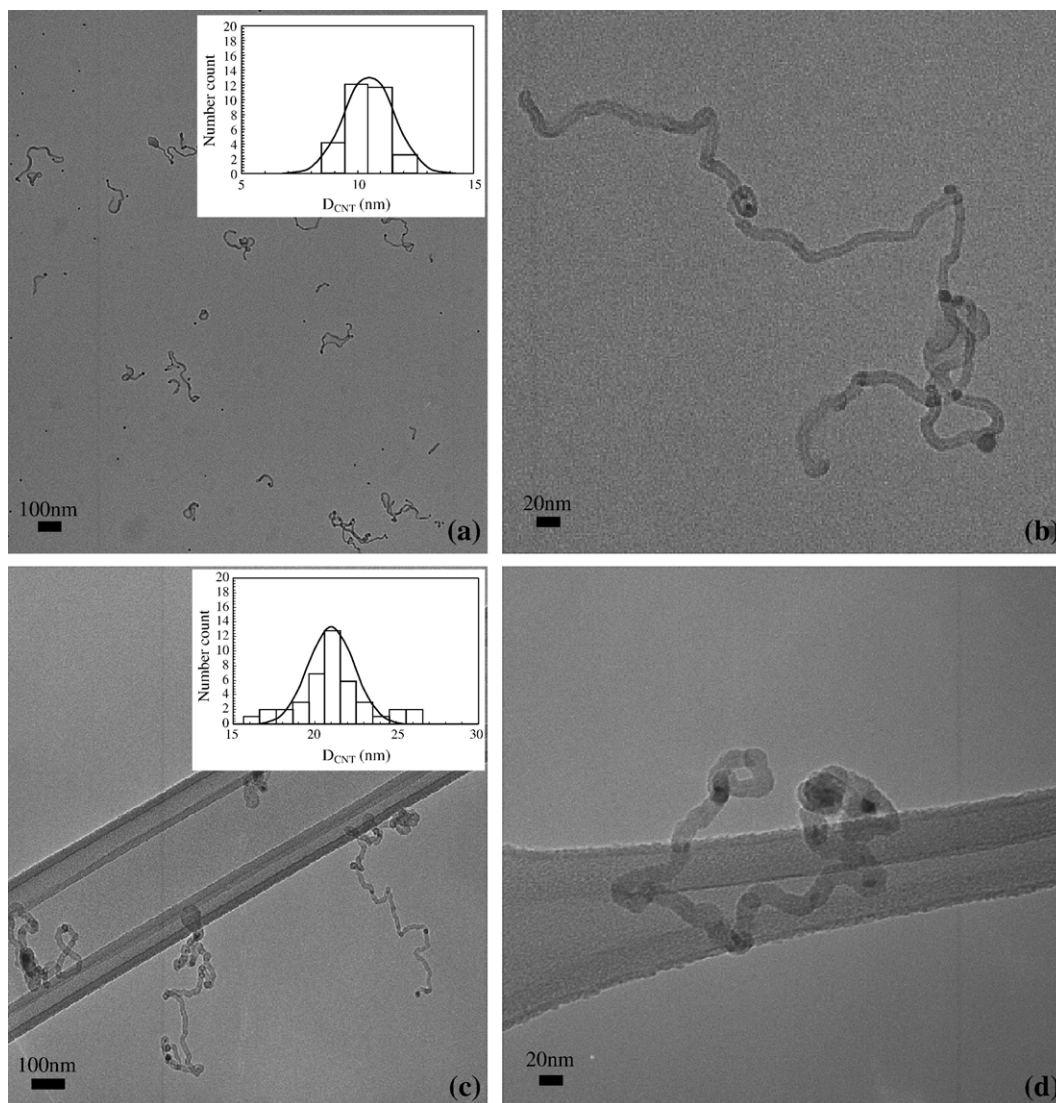


Fig. 4. TEM images of diameter-controlled CNTs grown on (a, b)  $D_m = 10$  nm and (c, d)  $D_m = 20$  nm of fully sintered nickel particles at 1200 °C. (a, c) are low resolution TEM images (the insert is the number count of CNTs as a function of CNTs' diameter ( $D_{\text{CNT}}$ )), (b, d) are high resolution TEM images.

The formation of spherical isolated metal particles is strongly dependent on the initial agglomerated particle size and sintering temperature, which we can track using tandem differential mobility analysis (TDMA, see Fig. 1) [12,18–20]. We use DMA-1 to select mono-area aggregated particles of 20, 32 and 52 nm mobility diameters. These particles are sent to the sintering reactor for known temperature and time and the resulting particles were then characterized by DMA-2. Since sintering results in a decrease in particle surface area and the DMA is an effective electrostatic band-pass particle area filter we can directly track the sintering kinetics. Fig. 3a shows the decrease in the mean mobility diameter with increasing temperature. The formation of single primary particles for the three different initial sizes employed requires temperatures of at least 1200 °C, which is very close to the melting point of bulk nickel ( $T_{m,Ni} = 1451$  °C). Shown in Fig. 3b are the resulting size distributions after sintering of the size-selected particles. Each initially selected aggregate size (labeled at peak in Fig. 3b) results in the very narrow size distributions with geometric standard deviations of less than  $\sim 1.2$ , indicating that the resulting nickel particles have monodisperse size distributions. The particle size distributions in Fig. 3b also show small satellite peaks. These correspond to the small fraction of particles that have two charges, and are therefore larger particles with the equivalent mobility diameter [12].

The free flowing stream of catalyst particles with a very narrow size distribution is then used to grow CNTs on-the-fly. For this experiment, the 10 and 21 nm size-selected and fully sintered nickel particles were passed to an aerosol flow reactor with an acetylene/hydrogen mixture at  $\sim 750$  °C. The total number concentration of size-selected nickel particles as measured by the DMA/CNC is  $\sim 10^5$  cm $^{-3}$ . With a nickel particle-laden flow rate of 1 lpm, this gives a total particle flow rate of  $\sim 10^8$  particles/min. TEM images of CNTs grown from the size-selected particles are presented in Fig. 4. Using digital image analysis software [21], the number distribution of CNTs as a function of CNT diameter could be determined. The histograms inserted in Fig. 4a and c present the diameter distribution for the CNTs grown on the size-selected nickel particles which show mean diameters of 10.5 and 21.0 nm with geometric standard deviations of  $1.08 \pm 0.02$  and  $1.14 \pm 0.03$ , respectively. These results indicate the continuous formation and deposition of diameter-controlled CNTs with a very narrow diameter distribution.

#### 4. Conclusion

We have demonstrated the gas-phase production of diameter-controlled CNTs, which is realized by controlling the diameter

of catalytic metal nanoparticles in the gas phase. The control of size and shape of catalytic particles grown in the gas phase was made by perturbing the competition between coagulation and sintering process, which was achieved by the use of gas-phase electrostatic separation and subsequent sintering process so that a monodisperse stream of catalytic nanoparticles were produced. These particles were then used in a continuous process to grow in-free-flight, narrow-diameter distribution CNTs.

#### References

- [1] S. Iijima, *Nature* 354 (1991) 56.
- [2] T. Guo, P. Nikolaev, A. Thess, D.T. Colbert, R.E. Smalley, *Chem. Phys. Lett.* 243 (1995) 49.
- [3] M. Glerup, H. Kanzow, R. Almairac, M. Castignolles, P. Bernier, *Chem. Phys. Lett.* 377 (2003) 293.
- [4] C.J. Lee, J. Park, J.A. Yu, *Chem. Phys. Lett.* 360 (2002) 250.
- [5] M.J. Bronikowski, P.A. Willis, D.T. Colbert, K.A. Smith, R.E. Smalley, *J. Vac. Sci. Technol., A, Vac. Surf. Films* 19 (4) (2001) 1800.
- [6] R. Andrews, D. Jacques, A.M. Rao, T. Rantell, F. Derbyshire, *Appl. Phys. Lett.* 75 (9) (1999) 1329.
- [7] T. Rueckes, K. Kim, E. Joselevich, G.Y. Tseng, C. Cheung, C.M. Lieber, *Science* 289 (2000) 94.
- [8] C.L. Cheung, A. Kurtz, H. Park, C.M. Lieber, *J. Phys. Chem., B* 106 (2002) 2429.
- [9] L. Ci, Y. Li, B. Wei, J. Liang, C. Xu, D. Wu, *Carbon* 38 (2000) 1933.
- [10] R.L. Vander Wal, T.M. Tichich, V.E. Curtis, *J. Phys. Chem., B* 104 (2000) 11606.
- [11] E.O. Knutson, K.T. Whitby, *J. Aerosol Sci.* 6 (1975) 443.
- [12] S.H. Kim, K.S. Woo, B.Y.H. Liu, M.R. Zachariah, *J. Colloid Interface Sci.* 281 (1) (2005) 46.
- [13] D. Chen, D.Y.H. Pui, *J. Nanopart. Res.* 1 (1999) 115.
- [14] S.N. Rogak, R.C. Flagan, H.V. Nguyen, *Aerosol Sci. Technol.* 18 (1993) 25.
- [15] J.H. Seinfeld, S.N. Pandis, *Atmospheric Chemistry and Physics*, John Wiley & Sons, Inc., 1998.
- [16] N.A. Fuchs, *Mechanics of Aerosols*, Pergamon, New York, 1964.
- [17] A. Kobata, K. Kusakebe, S. Morooka, *AIChE J.* 37 (1991) 347.
- [18] K.J. Higgins, H. Jung, D.B. Kittelson, J.T. Roberts, M.R. Zachariah, *J. Phys. Chem., A* 106 (2002) 96.
- [19] K.J. Higgins, H. Jung, D.B. Kittelson, J.T. Roberts, M.R. Zachariah, *Environ. Sci. Technol.* 37 (2003) 1949.
- [20] S.H. Kim, R.A. Fletcher, M.R. Zachariah, *Environ. Sci. Technol.* 39 (2005) 4021.
- [21] Image J, National Institutes of Health, <http://rsb.info.nih.gov/nih-image/>.